NASA Contractor Report 198175

ICASE Interim Report No. 27

ICASE

SOME DEVELOPMENTS OF THE EQUILIBRIUM PARTICLE SIMULATION METHOD FOR THE DIRECT SIMULATION OF COMPRESSIBLE FLOWS

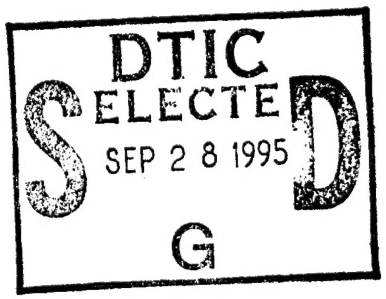

M. N. Macrossan

19950926 044

Contract No. NAS1-19480
June 1995

Institute for Computer Applications in Science and Engineering
NASA Langley Research Center
Hampton, VA 23681-0001

DTIC QUALITY INSPECTED 5

Operated by Universities Space Research Association

DISTRIBUTION STATEMENT A
Approved for public release;
Distribution Unlimited

Accesion For
NTIS CRA&I
DTIC TAB
Unannounced
Justification
By
Distribution /
Availability Codes
Dist | Avail and / or Special
A-1

Some Developments of the Equilibrium Particle Simulation Method for the Direct Simulation of Compressible Flows

M. N. Macrossan*
Lecturer, Department of Mechanical Engineering
University of Queensland, St. Lucia, 4072
Australia

Abstract

The direct simulation Monte Carlo (DSMC) method is the established technique for the simulation of rarefied gas flows. In some flows of engineering interest, such as occur for aero-braking spacecraft in the upper atmosphere, DSMC can become prohibitively expensive in CPU time because some regions of the flow, particularly on the windward side of blunt bodies, become collision dominated. As an alternative to using a hybrid DSMC and continuum gas solver (Euler or Navier-Stokes solver) this work is aimed at making the particle simulation method efficient in the high density regions of the flow. A high density, infinite collision rate limit of DSMC, the Equilibrium Particle Simulation method (EPSM) was proposed some 15 years ago. EPSM is developed here for the flow of a gas consisting of many different species of molecules and is shown to be computationally efficient (compared to DSMC) for high collision rate flows. It thus offers great potential as part of a hybrid DSMC/EPSM code which could handle flows in the transition regime between rarefied gas flows and fully continuum flows. As a first step towards this goal a pure EPSM code is described. The next step of combining DSMC and EPSM is not attempted here but should be straightforward. EPSM and DSMC are applied to Taylor-Couette flow with $Kn = 0.02$ and 0.0133 and $S_w = 3$). Toroidal vortices develop for both methods but some differences are found, as might be expected for the given flow conditions. EPSM appears to be less sensitive to the sequence of random numbers used in the simulation than is DSMC and may also be more dissipative. The question of the origin and the magnitude of the dissipation in EPSM is addressed. It is suggested that this analysis is also relevant to DSMC when the usual accuracy requirements on the cell size and decoupling time step are relaxed in the interests of computational efficiency.

*This research was supported by the National Aeronautics and Space Administration under NASA Contract No. NAS1-19480 while the author was in residence at the Institute for Computer Applications for Science and Engineering (ICASE), NASA Langley Research Center, Hampton, VA 23681-0001.

1 Introduction

The Direct Simulation Monte Carlo (DSMC) method [1] [2] is widely used for high speed rarefied gas flows for which the continuum equations of fluid mechanics are expected to be invalid. In this flow regime, the continuum gas properties such as density, flow velocity and temperature must be supplemented with information about the distribution of molecular energies amongst the molecules of the gas. In the case that the only relevant energies are those of translation and rotation of the molecules, the distribution function $f(\mathbf{v}, \varepsilon_{rot}, \mathbf{r}, t)$ is defined such that, at a given point $\mathbf{r}$ in the gas, at a given instant t, the expected number density (number/volume) of molecules which have a velocity in the range $\mathbf{v}$ to $\mathbf{v} + d\mathbf{v}$ and also have a value of rotational energy in the range ε_{rot} to $\varepsilon_{rot} + d\varepsilon_{rot}$ is given by $nfd\mathbf{v}d\varepsilon_{rot}$, where n is the number density of all molecules at the point.

In DSMC the molecules of a gas are represented by a very much smaller number of 'simulator particles'. The particles are first moved in collisionless trajectories for a small time interval Δt; then the particle velocities are subject to alteration during the collision phase of the calculation. The flow field is divided into small cells and representative collisions are calculated amongst the particles in each cell while conserving energy and momentum in each collision. The number of collisions calculated in each cell in each time step Δt reflects the appropriate local collision rate in the real gas. If the collision rate is large enough the distribution of the finite sample of particle velocities in a cell will conform (in a statistical sense) to the local Maxwell-Boltzmann equilibrium distribution f_0 (see equation (1)). If the collision rate is low there will be little re-distribution of molecular velocities and f will remain close to the value established in the cell by the free flight part of the simulation, and can thus be far removed from f_0.

In many blunt body atmospheric re-entry flows the gas near the windward surfaces of a spacecraft can be at a high density and the continuum fluid dynamics equations should apply, while the flow near the leeward surfaces is at a low density where DSMC should be used. It is appealing to use a particle method throughout these simulations rather than a hybrid DSMC/continuum code in which, to mention some apparent difficulties, the interface between the continuum and particle solvers could be bothersome [3] and the continuum solver might be adversely affected by the statistical noise generated by the DSMC calculations. The flow in the high density regions is collision dominated and, when using a particle method, prohibitively expensive amounts of CPU time can be spent calculating collisions. A suggestion by Bird [4] to limit the number of collisions in any cell in any time step to (say) 10 per particle has sometimes been used. The justification for this is that after 10 collisions per particle have been calculated the state in the cell will, in effect, be at equilibrium and more collisions cannot improve the accuracy of the simulation. However, even this collision limiting method can be prohibitively expensive.

The purpose of this work is to describe a high density version of DSMC which will be suitable for later use as part of a hybrid particle simulation code. The high density direct simulation method is called the Equilibrium Particle Simulation Method (EPSM) and was proposed by Pullin [5] as an infinite collision rate limit of DSMC for a single species of particle only but it contains all the necessary features of a method which can be easily combined with DSMC. In a hybrid DSMC/EPSM code the EPSM routines can be used to establish a new distribution of energies amongst the particles in those cells for which the theoretical

collision rate would require more than (say) 10 collisions per particle and this can be done without calculating any collisions at all in those cells. The two developments of EPSM which must be made before it can be suitable for a hybrid DSMC/EPSM code are

1. rotation energy must be handled in a manner compatible with existing DSMC codes and

2. multiple species of particles must be allowed for.

These two issues are addressed in sections (2) and (3).

A new code was constructed by replacing the collision routines in a freely available DSMC code with EPSM routines. The original code, called DSMC2A, was written by G. A. Bird [2] and can be obtained from the computer disk which accompanies ref. [2]. DSMC2A deals with a 2D axisymmetric flow in a rectangular region and has various options for setting boundary conditions and placing a surface within the flow; it allows for different species of molecules, any of which may possess energy of molecular rotation and vibration as well as translational energy. Some small coding errors in the original DSMC2A code were corrected. These are listed in Appendix B.

The new EPSM code is tested for Taylor-Couette flow and the results compared with the DSMC results obtained by repeating the DSMC calculations made at low Knudsen number by Stefanov and Cercignani [6] with the same grid size. It has been found that similar, but not identical, vortices will form using EPSM for which there is no attempt to model the collision rate (and hence the dissipation) correctly. The origin of the dissipation in EPSM is discussed in section 7; that discussion has some implications for DSMC when it is applied in the near continuum regime.

2 Vibration energy in EPSM

The Equilibrium Particle Simulation Method (EPSM) is similar to DSMC except that there is no calculation of molecular collisions. Instead, where DSMC would calculate collisions, it is assumed in EPSM that the collision rate is always large enough to bring about within a cell a distribution of particle velocities which represents (within the limitations set by the finite sample size) an approximation to an equilibrium distribution. For a single species of particle, with a particle mass m_s, for which rotation of the molecules (with two degrees of freedom) is active, the equilibrium distribution function is

$$f_0(\mathbf{v}, \varepsilon_{rot}) = \left(\frac{m_s}{2\pi k_b T}\right)^{\frac{3}{2}} \exp\left(\frac{-m_s(\mathbf{v}-\bar{\mathbf{v}})^2}{2k_b T}\right) \frac{1}{k_b T} \exp\left(\frac{-\varepsilon_{rot}}{k_b T}\right), \tag{1}$$

where k_b is Boltzmann's constant. The distribution of a single component of velocity, say v_x, can be obtained from (1) by performing the integration $\int_{-\infty}^{\infty}\int_{-\infty}^{\infty}\int_{0}^{\infty} f_0 dv_y dv_z d\varepsilon_{rot}$. The result is

$$f_u(v_x) = \left(\frac{m_s}{2\pi k_b T}\right)^{\frac{1}{2}} \exp\left(\frac{-m_s(v_x-\bar{v}_x)^2}{2k_b T}\right) \tag{2}$$

Thus a single component of molecular velocity is normally distributed in an equilibrium gas.

EPSM bypasses the calculation of a large number of collisions amongst the finite sample of particles in each cell by selecting the new velocity components from a normal distribution in such a way that the mean and variance of the finite sample conform to values determined by the requirement that the total energy and momentum be conserved in each cell. This problem is different from the simpler problem of generating a finite sample of velocities selected from a parent distribution which has a known mean and variance. That is, because of the finite sample of simulator particles which are used in any simulation (or any ensemble of simulations) the values of $\bar{\mathbf{v}}$ and T in (1) are not known exactly in EPSM or DSMC; what is known is the estimate of these quantities which are derived from the finite sample. Thus the estimate of the macroscopic fluid velocity, the mass average particle velocity $\bar{\mathbf{v}}_{est}$, is given by

$$\bar{\mathbf{v}}_{est} = \sum_{k=1}^{N} m_k \mathbf{v}_k / M_{tot} \tag{3}$$

where N is the number of particles in the sample, m_k is the mass of the k-th particle in the sample and

$$M_{tot} = \sum_{k=1}^{N} m_k \tag{4}$$

is the total mass of the N particles. The estimate of the temperature, T_{est}, is derived from the total energy of the finite sample of N particles. It is related to the average thermal energy per single degree of freedom for a single particle, $e'_{d.o.f.}$ (see equation (11)), by

$$e'_{d.o.f} = \frac{1}{2} k_b T_{est}. \tag{5}$$

In the original application of EPSM [5] a one dimensional flow of a single species of particle was treated. The mathematical derivation of a procedure for selecting velocity components which are normally distributed and are constrained to have a specified mean and variance was developed in [7]. The procedure is given in the form of an algorithm in [5]; the algorithm is also given here in Appendix A but in greater detail, particularly for the special cases when the number of velocities to be set is low.

In the original application of EPSM [5] energy of molecular structure, such as rotation, was not assigned to individual particles in the simulation but rather the total energy of molecular structure was calculated by assuming each degree of freedom contained exactly the same thermal energy as was contained in a single translational degree of freedom[†]. In current DSMC codes energy of molecular rotation is assigned to each particle, and for compatibility with these codes the EPSM code developed here allows for molecular rotation energy as described below. The code can be easily generalized to any number of fully excited (classical) degrees of freedom but the issue of treating vibration energy which is not fully excited is not dealt with here.

It is convenient to represent molecular rotation in two degrees of freedom by a pseudo-velocity having two components (μ_1, μ_2), where

$$\varepsilon_{rot} = \frac{1}{2} m_s \left({\mu_1}^2 + {\mu_2}^2 \right). \tag{6}$$

[†]In fact a similar argument was applied to the energy stored in the two redundant velocity components which then did not have to be stored for the one dimensional flow case.

Then, in an equilibrium state, the distribution function is given by

$$f_0\left(v_x, v_y, v_z, \mu_1, \mu_2\right) = \left(\frac{m_s}{2\pi k_b T}\right)^{\frac{5}{2}} \exp\left(\frac{-m_s\left(v'_x{}^2 + v'_y{}^2 + v'_z{}^2 + \mu_1{}^2 + \mu_2{}^2\right)}{2k_b T}\right) \tag{7}$$

where $v'_x = v_x - \bar{v}_x$, $v'_y = v_y - \bar{v}_y$, $v'_z = v_z - \bar{v}_z$ are the three components of *thermal* velocity. If an approximation to the equilibrium distribution (7) can be established in a cell the two components of pseudo-velocity can be converted to a single value of rotational energy ε_{rot} which is stored for each particle. It follows from (6) and (7) that the distribution of ε_{rot} so derived will conform to (1).

3 Multiple species

The EPSM code used here was derived by replacing the collision routines in DSMC2A (subroutines COLLMR, SELECT2A, ELASTIC, INELR and LBS) with a subroutine which, for all cells, first determines the mass averaged velocity and thermal energy of all the particles in the cell. Then for each degree of freedom for each species of particle a new subroutine EQUIL (which executes the algorithm in Appendix A) is called in order to establish the new distribution of energy in the single degree of freedom amongst all the particles of the species. In so doing the mean velocity of each species is constrained to be exactly equal to the mass averaged velocity and the random energy stored in each degree of freedom is the same for each species and for each degree of freedom. Some implications of this are discussed in section (4).

The input to the EQUIL subroutine is the number of particle velocities to be set N_s, the required mean velocity of the single component of velocity $\bar{u}$, and e' which is the total specific thermal energy stored in the single degree of freedom divided by the mass of one particle. Thus after the N_s particle velocities have been set (for particles all having the same molecular mass) we have

$$\bar{u} = \frac{1}{N_s}\sum_{j=1}^{N_s} u_j \tag{8}$$

and

$$e' = \frac{1}{2}\sum_{j=1}^{N_s}\left(u_j - \bar{u}\right)^2. \tag{9}$$

Note that u may be any one of the three components of molecular velocity (v_x, v_y, v_z) or a pseudo-velocity component representing a single degree of freedom for rotation, in which case $\bar{u} = 0$.

The required value of e' is determined before each call to EQUIL from

$$e' = N_s e'_{d.o.f.}/m_s \tag{10}$$

where m_s is the particle mass and $e'_{d.o.f}$ is the mean thermal energy per single degree of freedom given by

$$e'_{d.o.f.} = E'/\nu. \tag{11}$$

In (11), E' is the total thermal energy of all particles in the cell and ν is the total number of degrees of freedom. The latter is given by

$$\nu = \sum_{k=1}^{N} (3 + \xi_k) . \tag{12}$$

where ξ_k is the number of fully excited (classical) degrees of freedom of the molecular structure; thus $\xi = 0$ for monatomic particles such as argon and helium and $\xi = 2$ for diatomic species such as nitrogen and oxygen at room temperatures.

In order to determine the total thermal energy E', the total translational energy E_{tr} of the N particles in the cell must be divided into the bulk translational energy and the random thermal energy relative to the bulk motion. The thermal velocity[‡] of the *k-th* particle is defined by

$$\mathbf{v'}_k = \mathbf{v}_k - \bar{\mathbf{v}}_{est}. \tag{13}$$

It follows from (3) and (13) that

$$\sum_{k=1}^{N} m_k v'_{x_k} = \sum_{k=1}^{N} m_k v'_{y_k} = \sum_{k=1}^{N} m_k v'_{z_k} = 0. \tag{14}$$

The total translational energy of the N particles is given by

$$E_{tr} = \frac{1}{2} \sum_{k=1}^{N} m_k \mathbf{v}^2{}_k = \frac{1}{2} \sum_{k=1}^{N} m_k \left(v^2_{x_k} + v^2_{y_k} + v^2_{z_k} \right) . \tag{15}$$

By expressing the velocity of each particle in terms of the mass average velocity and thermal velocity (15) may be written as

$$\begin{aligned} E_{tr} &= \frac{1}{2} \sum_{k=1}^{N} m_k \left(\left(\bar{v}_x + v'_{x_k} \right)^2 + \left(\bar{v}_y + v'_{y_k} \right)^2 + \left(\bar{v}_z + v'_{z_k} \right)^2 \right) \\ &= \frac{1}{2} \sum_{k=1}^{N} m_k \left(\bar{v}^2_x + \bar{v}^2_y + \bar{v}^2_z \right) + \frac{1}{2} \sum_{k=1}^{N} m_k \left(v'^2_{x_k} + v'^2_{y_k} + v'^2_{z_k} \right) \\ &\quad + \bar{v}_x \sum_{k=1}^{N} m_k v'_{x_k} + \bar{v}_y \sum_{k=1}^{N} m_k v'_{y_k} + \bar{v}_z \sum_{k=1}^{N} m_k v'_{z_k} \\ &= \frac{1}{2} M_{tot} \bar{\mathbf{v}}^2_{est} + E'_{tr} \end{aligned} \tag{16}$$

where use has been made of the (14) and where

$$E'_{tr} = \frac{1}{2} \sum_{k=1}^{N} m_k \mathbf{v'}_k{}^2 \tag{17}$$

is the total translational thermal energy in the cell. The total energy of the particles is $E_{tot} = E_{tr} + E'_{rot}$, that is, it includes thermal energy stored in the rotation of the particles. The total thermal energy (*translation + rotation*) is given by

$$E' = E'_{tr} + E'_{rot} = E_{tot} - \frac{1}{2} M_{tot} \mathbf{v}^2 . \tag{18}$$

[‡]Strictly speaking, $\mathbf{v'}$ is the estimated thermal velocity of a particle; that is, it is the velocity relative to the simulation estimate of the true gas velocity at that cell's location.

4 Some comments on EPSM and DSMC

It might be thought that another method of setting the equilibrium state within each cell could be used. Given that the estimates of the mean velocity and the temperature in each cell are known from (3) and (5), a set of equilibrium particle energies could be selected directly from the distribution (1) with $\mathbf{v} = \bar{\mathbf{v}}_{est}$ and $T = T_{est}$, in exactly the same way that an initial equilibrium state of a gas is set in standard DSMC. However in that case, the mean velocity of the finite sample so selected will not equal $\bar{\mathbf{v}}_{est}$ and the mean thermal energy of the finite sample of velocities will not correspond to T_{est}; in other words, momentum and energy will not be exactly conserved by the redistribution. Nanbu's simulation method [8] is another direct simulation method that does not conserve momentum and energy exactly in collisions, and this seems to be the cause of the greater statistical scatter in the results compared with DSMC [9] [10]. It seems highly likely that the above procedure for setting an equilibrium state without preserving momentum and energy exactly would be unsatisfactory as well.

The EPSM procedure does more than conserve energy as the new state in a cell is established. By setting each degree of freedom separately as described in section (3) the final state is slightly different from the state that would be established in DSMC after a large number of collisions had been calculated. In the DSMC equilibrium state the mean velocity of each species would be approximately, but not exactly, the same as the mass averaged velocity and the different degrees of freedom would not contain exactly the same thermal energy. There is some indication in the results that follow that EPSM shows less variation than DSMC between different runs (using a different sequence of random numbers) for the same flow. This may be related to the slightly less statistical variation that is allowed in EPSM when the velocity distribution function is represented by a finite sample of particle velocities.

The EPSM algorithm could be used to set the initial state in DSMC in which case the initial state would contain an exact specified amount of energy and each degree of freedom would contain exactly the same total amount of thermal energy. It is possible that this might reduce the statistical scatter in DSMC calculations somewhat, particularly when data are obtained by averaging over an ensemble of different runs; in standard DSMC the nominally identical initial states contain slightly different total amounts of energy and momentum. It might also be possible, and useful, for something similar to be done to establish incoming fluxes at flow boundaries. In DSMC a selection of particles from an equilibrium gas flows into the simulation and this selection contains a statistically varying amount of energy and momentum at each step, even though the boundary condition is fixed; it might be preferable if exactly the same energy and momentum was carried in at each step (while the individual particle velocities varied between steps).

5 Computational Efficiency of EPSM *vs.* DSMC

The expected use of EPSM as part of a hybrid DSMC/EPSM code requires that EPSM be more efficient than DSMC for establishing equilibrium. In this section the computational efficiency of EPSM is investigated. In a hybrid code EPSM will only be used where the

standard DSMC procedures call for a large number of collisions to be calculated in a single time step. This can only happen if the normal requirement that Δt be small with respect to the local collision time is relaxed, at least in some part of the flow. If this criteria is not relaxed it follows that the average number of collisions per particle will be less than 1 and it would be inappropriate to use EPSM in such a situation unless it were known in advance that an equilibrium state existed in the cell. There are situations where large cell sizes are used in regions of flow where the flow gradients are small, and in that case the time step could be large relative to the local collision time. This is particularly likely to happen for multi-grid applications of DSMC.

In order to compare computational efficiency, DSMC and EPSM have been used to simulate a gas at rest throughout the region between two stationary cylinders. The gas conditions were the same as the initial state considered in section (6) for Taylor-Couette flow. The expected result is that the flow remain in its initial state (in a statistical sense) for all values of the time step, and this was realized. The timing results are shown in figure (1). For values of $\Delta t\sqrt{2RT_1}/\lambda_1 = 10$, for which the number of collisions per particle per time step is approximately 10, EPSM requires approximately 30% of the CPU time required by DSMC. Thus EPSM is an excellent alternative to DSMC in those cells in which many collisions must be calculated in one time step. It should also be noted that not a great deal of attention has yet been paid to considerations of computational efficiency in EPSM; there is probably more room for improvement.

6 EPSM applied to Taylor-Couette Flow

In order to demonstrate the use of EPSM an interesting vortical flow (Taylor-Couette flow) has been considered, even though the particular conditions considered are not necessarily those for which for which EPSM will be as accurate as DSMC. The classical case of Taylor-Couette flow occurs when a gas is contained between two coaxial cylinders of infinite length and the inner cylinder rotates while the outer cylinder is at rest. At low rotation speeds, a laminar flow is induced between the cylinders; this is an axisymmetric version of the familiar laminar Couette flow between two plates which move relative to each other. For higher rotational speeds a number of toroidal vortices will develop. At even higher rotational speeds the vortices can break down and the flow can become fully turbulent and three dimensional. Here axisymmetric flow only is considered; three velocity components are carried with the particles in the simulation (as is usual for DSMC) and the boundary condition at the surface of the rotating cylinder imparts a tangential velocity to the particles. Figure (2) shows the computational domain and an example of a time averaged EPSM flow with typical vortices.

Stefanov and Cercignani [6] made a through study of this flow for a moderately rarefied gas and Bird [2] has repeated one of their calculations. Here both EPSM and DSMC simulations have been performed. For DSMC the molecular model is a hard sphere with the molecular size appropriate to Argon at a temperature of 273 K [2]. The ordinary gas constant is $R = k_b/m = 208.2\, J\, kg^{-1}K^{-1}$. Argon has no rotational or vibrational energy and thus the ratio of specific heats is $\gamma = 5/3$.

The inner cylinder radius was 0.025 m and the outer cylinder radius was 0.05 m so that the gap between the cylinders was $\Delta R = 0.025$ m. The simulations began with a uniform

gas at rest between the cylinders and the rotation of the inner cylinder began impulsively. The initial gas state was given by $T_1 = 273\ K$, and two values of initial density ρ_1 were used:

1. $\rho_1 = n_1 m = 1.716 \times 10^{-4}\ kg\ m^{-3}$, $P_1 = 0.130 \times 10^5\ Pa$, $\lambda_1 = 5 \times 10^{-4} m$ and
2. $\rho_1 = n_1 m = 2.574 \times 10^{-4}\ kg\ m^{-3}$, $P_1 = 0.195 \times 10^5\ Pa$, $\lambda_1 = 3.33 \times 10^{-4} m$.

The tangential speed of the inner cylinder wall was $1011.33\, ms^{-1}$. The inner and outer cylinder surface temperatures were constant at $T_w = T_1$ and diffuse reflection was assumed. In the axial direction the simulation region had a length of $L = 4\Delta R$ and was bounded by specularly reflecting surfaces at each end.

For the given geometry the flow can be characterized by three non-dimensional parameters

1. the Knudsen number based on the gap between the cylinders, $Kn = \lambda_1/\Delta R = 0.02$ or 0.0133,
2. the speed ratio $S_w = V_w/\sqrt{2RT_1} = 3$, where V_w is the tangential speed of the inner cylinder and
3. the wall to gas temperature ratio $T_w/T_1 = 1$.

Different grids were used for the different Knudsen number flows; in both cases the cells were square with sides equal to λ_1 and the decoupling interval (time step) was set as $\Delta t = \frac{2}{3}\lambda/\sqrt{2RT_1}$. Variable weighting factors were not used so the number of simulator particles remained constant throughout the simulation. It must be remembered that the EPSM simulations are independent of the collision rate (in effect the collision rate is infinite) and hence do not depend on the Knudsen number. The EPSM results may depend on the number of simulator particles used, the cell size and the decoupling interval. Some of these issues are addressed in section (7) which deals with the nature of the dissipation inherent in EPSM.

The flow can be visualized with the aid of stream traces constructed from the velocity field in the $x - r$ plane. Each drawing of these vortices used the same number and starting locations of the stream traces. Each figure shows the normalized time $\hat{t} = tV_w/(2\pi R_{inner})$ at the end of the sampling period. Except where explicitly stated in the caption the figures show results of averaging the flow over a single revolution of the inner cylinder.

Comparison of DSMC and EPSM results gives an indirect method of determining how closely the DSMC calculations are approaching the equilibrium limit or how well the DSMC simulations represent the small departures from equilibrium which might be expected for small but non-zero Knudsen numbers. If the DSMC results were no different, or little different, from the EPSM results it would mean that the state in each cell was, in effect, in local equilibrium; it would then have to be considered whether this could be a valid result for this flow. If the results for EPSM and DSMC are different then it must be concluded that EPSM is not suitable for the case considered; this sort of information will be useful to determine the appropriate regime of application of EPSM in any hybrid DSMC/EPSM code. The question of the accuracy of the DSMC results depends on the usual requirements that the cell size and decoupling time step be small relative to the mean free path and collision time, respectively; these requirements are approximately, but not unambiguously, satisfied in these simulations.

It was found that EPSM required about 10% more CPU time than DSMC in these simulations. This is what can be expected according to figure (1) for the value of Δt used. This emphasizes the point that where the usual accuracy requirements can be met (or approximately met), EPSM is, in theory, not only inferior (to an unknown extent) to DSMC but is also inefficient (at present) compared with DSMC; it is only where the usual requirements are relaxed, and the number of collisions per particle per cell becomes greater than 1 that EPSM is more efficient than DSMC and becomes strictly justified on the grounds that DSMC approaches the EPSM limit.

6.1 Results for 200×50 grid. $Kn = 0.02$

This grid is the same as that used in [2]. The flow was sampled at intervals of $3\Delta t$ so an average particle in the undisturbed gas would move approximately 2 cell widths between samplings. In the time required for a single revolution of the inner cylinder the flow was sampled 52 times.

The unsteady development of the flow calculated using EPSM is shown in figures (3), (4) and (5). At first there are four vortices which reduce to three after 10 revolutions and the sizes of the vortices vary with time. The development of the flow using DSMC is shown in figures (6), (7) and (8). DSMC gives a very different result from EPSM; there are five or six vortices rather than three. This is also different from the DSMC result of Bird [2], which contained three vortices, and of Stefanov and Cercignani [6], which contains four vortices. A DSMC flow is not exactly reproducible between runs and the same applies to an EPSM flow; both methods depend on the sequence of random numbers used in the simulation. Apparently DSMC is particularly sensitive to this effect [11] for this vortical flow.

These calculations were repeated for both EPSM and DSMC using a different sequence of random numbers and the results after twenty revolutions are shown in figures (9) and (10); these can be compared with those shown in figures (5) and (8). Three vortices developed for all EPSM calculations made for this case, some of which continued for sixty revolutions. On the other hand, only four vortices developed for DSMC in this new run. The DSMC calculations used four sub-cells for each of the 50x200 cells in the grid[§] and this gives an average of only three particles per sub-cell which seems a very small sample from which to be choosing collision partners; this small number of particles in each sub-cell may well be the source of the larger variation between runs for DSMC than for EPSM. The EPSM procedure was implemented over the entire cell; a better comparison between EPSM and DSMC could be made if EPSM were also implemented at the sub-cell level, which has not yet been done. It is worth noting that only about four particles per cell where used in Stefanov and Cercignani's simulations [6] which also differ from the DSMC results here.

6.1.1 Larger number of simulator particles

This case ($Kn = 0.02$, 50x200 grid) was re-calculated using twice the number of simulator particles for both EPSM and DSMC. Two different EPSM results are shown in figures (11) and (12). There is some difference between these results and each differs from the EPSM

[§]Collision partners are selected from the same sub-cell while the collision rate for the entire cell, not the individual sub-cells, is correctly simulated for the conditions averaged over the entire cell [2].

result found with a smaller number of simulator particles for which there were three rather than the five or six vortices shown here. For DSMC there is a much bigger effect when the number of simulator particles is doubled; no vortices at all are formed (see figures (13) and (14)).

On the assumptions

1. that DSMC gives a better realization of this flow than EPSM does and
2. that increasing the number of simulator particles increases the accuracy of the simulation

(two assumptions that can hardly be doubted) there is a trend that the vortices become smaller (or disappear) as the accuracy increases. It might be that the simulation becomes less dissipative as it becomes more accurate and that more vortices develop for a less dissipative flow (in effect a higher Reynolds number flow) and eventually the vortices become unstable at sufficiently high Reynolds number. However, to exclude what seems a remote possibility, that the results for DSMC in this case correspond to a laminar flow with statistical noise, a detailed statistical analysis along the lines of that done in [6] would be necessary.

The question of dissipation in EPSM is addressed in section (7); it is not immediately clear exactly how the number of simulator particles N_{tot} is related to the dissipation in these methods, (although for partcile simulation methods the random noise $\sim 1/\sqrt{N_{tot}}$ [2]).

6.2 Results for 300×75 grid. $Kn = 0.0133$

Both EPSM and DSMC simulations were repeated for a higher density flow and with a smaller cell size. The decoupling interval was such that $\Delta t\sqrt{2RT_1}/\lambda_1$ remained at 0.67. The total number of particles was twice that for the 50x200 grid and the average number of particles per cell was 10.6, slightly less than the minimum on the 50x200 grid (11.9 particles per cell). The DSMC results would be expected to change for this different physical situation and the EPSM results would also be expected to change since, if the argument in section (7) is correct, the effective viscosity (effective mean free path) in EPSM depends on the cell size and decoupling interval.

The unsteady development of the flow for EPSM is shown in figures (15), (16) and (17). This can be compared with the DSMC flow shown in figures (18), (19) and (20). For EPSM there is not much difference at $\hat{t} = 20$ between the vortices in figure (17) for $Kn = 0.0133$ and those in figure (9) for $Kn = 0.02$. and for DSMC there is not much difference between figure (20) for $Kn = 0.0133$ and figure (10) for $Kn = 0.02$. Of course a greater difference can be found by comparing with the low density runs of DSMC for which five vortices (or no vortices at all!) formed. If the purpose of this work were to investigate this Taylor-Couette flow in detail or to investigate fully the sensitivity of DSMC in this application it would obviously be desirable to repeat this low Knudsen DSMC calculation with a larger number of simulator particles; it could well be that the vortices disappear as they did for the higher Knudsen number case.

While it is difficult to draw any firm conclusions about the Taylor-Couette flow from these results it is interesting to note that the DSMC results are different enough from the EPSM results (five vortices rather than three) to suggest that the velocity distribution function f

may be significantly different from equilibrium in these simulations even though the Knudsen number at 0.0133 is 'small'. However it must be remembered that the product $S_w Kn$ is more relevant than Kn alone. The former may be expressed as

$$S_w Kn \approx \frac{\lambda}{(2RT_1)^{\frac{1}{2}}} / \frac{\Delta R}{V_w} \approx \frac{V_w \lambda}{(2RT_1)^{\frac{1}{2}}} / \Delta R \tag{19}$$

and is thus a ratio of

1. a characteristic time between collisions $t_{coll} = \lambda / (2RT_1)^{\frac{1}{2}}$ and a characteristic time of the macroscopic flow $\Delta R / V_w$ or

2. a characteristic distance $V_w t_{coll}$ traveled (in the laboratory reference frame) by the molecules between collisions and a characteristic dimension of the macroscopic flow ΔR[¶].

While the usual definition of mean free path, the distance traveled between collisions measured in a frame of reference moving with the local fluid velocity, makes it a convenient state property that combines the gas density, temperature and molecular size, it is not necessarily the most appropriate microscopic length scale for high speed flows, as should become apparent after writing the Boltzmann equation in non-dimensional form (see for example [12]). It seems unfortunate that the term 'mean free path' can not be used to refer to the distance between collisions measured in the whatever reference frame is relevant to the flow; if it could, the term 'mean free path' might be better applied to

$$\Lambda = V_{char} t_{coll} \tag{20}$$

where

$$V_{char} = \max \left[V_{fluid}, (2RT_{char})^{\frac{1}{2}} \right]$$

is a characteristic speed based on either the macroscopic flow speed or a characteristic thermal speed of the molecules. Equation (20) may be written as

$$\Lambda = \max [1, S_w] \, \lambda$$

where λ is the mean free path as conventionally defined. The mean collision time t_{coll} or its inverse could serve as a state property which carries information about the gas state only, just as well as λ can.

7 Effective mean free path and dissipation in EPSM

EPSM is an infinite collision rate limit of DSMC with a finite sample of simulator particles. The 'infinite particle' limit of EPSM is known as the Equilibrium Flux Method (EFM)[‖] [5]

[¶]It is also the ratio of a characteristic shear stress in the flow, $\mu_1 V_w / \Delta R$, and a characteristic pressure, $\rho_1 RT_1$ and it may be written as $\approx M^2 / Re$, where M is the Mach number and Re is the Reynolds number.

[‖]Not an exact limit, since some gradient information in EPSM carried by the possible non-uniform spatial distribution of particles in a cell is absent from EFM. Pullin's EFM has has been rediscovered in [13] and given a new acronym (KFVS). Here I follow the convention that the naming rights belong to the originator of the method.

and has been used as an Euler flow solver in its first order [14] [15] [16] [17] and second order [18] [19] [20] formulations and as the basis of a Navier-Stokes solver [21] [22] [23]. The dissipation inherent in EFM has been demonstrated for a special case [15] and can be evaluated more generally [24]. It is worth reviewing those demonstrations since they shed light on the nature of the dissipation which arises in EPSM and, in some circumstances, in DSMC.

If the decoupling interval (or time step Δt) in EPSM is set to a value larger than the time of flight across a typical cell then a typical particle will move to a new cell carrying with it momentum and energy which are representative of the conditions in the cell from which it came. Next its momentum and energy is transmitted to its new cell as it undergoes, in effect, an infinite number of collisions with all the other particles in the cell. Clearly the distance traveled between collisions in EPSM (and in DSMC) cannot be less than the distance traveled by a typical particle in time Δt. This corresponds to a minimum mean free path (as conventionally defined in the reference frame moving with the mean flow velocity) of approximately $(8RT/\pi)^{\frac{1}{2}}\,\Delta t$.

On the other hand, consider the case where Δt is small so that the chance that particles will cross more than one cell in any one time step is negligible. Consider two adjacent cells in an EPSM simulation as shown in figure (21). Let a local set of axes $(\hat{\mathbf{n}}, \hat{\mathbf{p}}, \hat{\mathbf{q}})$ be attached to the interface and let $\hat{\mathbf{n}}$ point from the cell denoted $(+)$ to the cell denoted $(-)$. Let v_n, v_p, v_q be the components of molecular velocity with respect to the local axes. All particles having $c_n > 0$ which cross the interface are selected from the equilibrium distribution f_0^+ established in the $(+)$ cell; all particles crossing the interface having $c_n < 0$ are selected from a different equilibrium distribution f_0^-. As a result the distribution of c_n of those particles which cross the interface is discontinuous at $c_n = 0$ as shown in the figure.

It is to be expected that the fluxes derived from this (discontinuous, non-equilibrium) distribution of velocities of those particles crossing the interface will contain parts corresponding not only to the continuum Euler fluxes (for a hypothetical equilibrium state at the interface) but extra 'dissipative' fluxes. Note that figure (21) shows a hypothetical equilibrium distribution derived from the non-equilibrium distribution; the full set of dissipative fluxes for EPSM (relative to this hypothetical equilibrium distribution) is given in [24] and these results could be used to derive an effective mean free path for EPSM. Here, to illustrate the point, a simple example of the exchange of fluxes between cells in EPSM is considered.

7.1 Fluxes in EPSM

Let Q be one of the molecular properties $m, m\mathbf{v}$ or $m\left(\frac{1}{2}\mathbf{v}^2 + \varepsilon_{rot}\right)$ (mass, momentum and energy) which are transported as the particles move. The net flux (/unit area/unit time) of Q across the interface can be split into two parts: a forward flux F_Q^+ which flows in the direction of $\hat{\mathbf{n}}$ and a backward flux F_Q^- which flows in the opposite direction. The total flux is

$$F_Q = F_Q^+ + F_Q^- \tag{21}$$

where the two parts of the fluxes can be obtained from standard kinetic theory (*e.g.* [2]) as

$$F_Q^+ = \int_{-\infty}^{\infty}\int_{-\infty}^{\infty}\int_{0}^{\infty} n^+ f_0^+ Q v_n dv_n dv_p dv_q \tag{22}$$

and

$$F_Q^- = \int_{-\infty}^{\infty}\int_{-\infty}^{\infty}\int_{-\infty}^{0} n^- f_0^- Q v_n dv_n dv_p dv_q. \tag{23}$$

In (22) and (23), $n = \rho/m$ is the number density of particles and m is the mass of one particle.

Now consider the idealized situation in figure (22) which shows adjacent cells in a section of the flow where there the gradient $\partial v_p/\partial x_n \neq 0$ To evaluate the net transfer of p-momentum across the interface we need to put $Q = mc_p$ and perform the integrations in (22) and (23). With the form of f_0^+ and f_0^- known from (1) the forward and backward fluxes of p-momentum are

$$F_{mv_p}^{\pm} = W^{\pm}\rho^{\pm}v_n^{\pm}v_p^{\pm} \pm D^{\pm}\rho^{\pm}\left(2RT^{\pm}\right)^{\frac{1}{2}} v_p^{\pm} \tag{24}$$

where

$$W^{\pm} = \frac{1}{2}\left[1 \pm \operatorname{erf}\left(s_n^{\pm}\right)\right], \tag{25}$$

$$D^{\pm} = \pm\frac{1}{2\pi^{\frac{1}{2}}}\exp\left[-\left(s_n^{\pm}\right)^2\right]. \tag{26}$$

and

$$s_n^{\pm} = v_n^{\pm}/\left(2RT^{\pm}\right)^{\frac{1}{2}}. \tag{27}$$

If we further assume there are no gradients other than $\partial v_p/\partial x_n$, we have $\rho^+ = \rho^- = \rho$, $v_n^+ = v_n^- = v_q^+ = v_q^- = 0$ and $T^+ = T^- = T$, and the net flux (/unit area/unit time) of p-momentum across the interface is

$$F_{mv_p} = \rho\left(RT/2\pi\right)^{\frac{1}{2}}\left(v_p^+ - v_p^-\right). \tag{28}$$

This net flux is the shear stress τ acting at the interface and, since $\left(v_p^+ - v_p^-\right)$ may be approximated by $\Delta x_n \partial v_p/\partial x_n$ where Δx_n is the cell size, we have

$$\tau = \rho\left(RT/2\pi\right)^{\frac{1}{2}}\Delta x_n \partial v_p/\partial x_n. \tag{29}$$

Comparing this to the stress-strain relationship for plane Couette flow, $\tau = \mu\left|\partial v_p/\partial\right| x_n$, we get the effective viscosity for EPSM as

$$\mu' = \left(RT/2\pi\right)^{\frac{1}{2}}\rho\Delta x_n. \tag{30}$$

Comparing this to the usual relation between mean free path and viscosity

$$\mu \approx \frac{1}{2}\rho\left(8RT/\pi\right)^{\frac{1}{2}}\lambda$$

we obtain an effective mean free path in EPSM of

$$\lambda' \approx \Delta x_n/2. \tag{31}$$

Combining the results for $\Delta t > \Delta x/\bar{v}$ and $\Delta t < \Delta x/\bar{v}$ where Δx is a characteristic cell size and $\bar{v}$ is the magnitude of the local mean particle velocity (mean fluid velocity) we can say that there is an effective mean free path in EPSM given by

$$\begin{aligned} \lambda_{EPSM} &\approx \max\left[\frac{1}{2}\Delta x, (8RT/\pi)^{\frac{1}{2}}\Delta t\right] \\ &\approx \frac{1}{2}\max\left[1, \frac{4}{\pi^{\frac{1}{2}}}\frac{C}{S}\right]\Delta x \end{aligned} \tag{32}$$

where $C = \bar{v}\Delta t/\Delta x$ is the CFL number and $S = \bar{v}/(2RT)^{\frac{1}{2}}$ is the local speed ratio. We could also say that the effective viscosity in EPSM is given by

$$\mu_{EPSM} \approx \max\left[1, \frac{4}{\pi^{\frac{1}{2}}}\frac{C}{S}\right](RT/2\pi)^{\frac{1}{2}}\rho\Delta x. \tag{33}$$

7.2 Implications for DSMC

The above analysis applies approximately to DSMC and becomes more exact as the distribution function approaches an equilibrium form. Hence the effective mean free path in DSMC would be given by

$$\lambda_{DSMC} = \max\left[O\left(\Delta x_n\right), \lambda\right]$$

where λ is the local mean free path for the molecular collision model being used. This is merely another way of stating the theoretical requirement that the cell size in DSMC should be less than λ. It is worth noting, however, that the effective viscosity in DSMC will be given by an expression similar to (30) and not by the theoretical viscosity of the molecular collision model, when the cell size is larger than λ, as may be the case when it is based on a (larger) local characteristic length derived from flow gradients. In other words, the collision model is largely irrelevant when the cell size is large, and in that case EPSM is probably little different from DSMC.

It is obvious that DSMC and EPSM should give similar results when the number of collisions per particle per time step in DSMC is large, which is likely to be the case when cell sizes, and hence the decoupling interval, are large. This does not necessarily imply an inadequacy in DSMC or EPSM, since when flow gradients are small and large cell sizes are used, the local flow state is most likely to be very close to equilibrium. An analogy in continuum fluid mechanics is that the Euler equations (rather than the full Navier-Stokes equations) can give reasonable results in regions of the flow where gradients are small.

8 Conclusions

The equilibrium particle simulation method (EPSM) [5] has been extended to handle flows with multiple species and multiple (classical) degrees of freedom of molecular structure. EPSM is now a suitable method to be used as the high density part of a hybrid particle simulation method for flows which contain regions of rarefaction as well as regions of near continuum flow. EPSM cannot be expected to be used as an alternative to DSMC for all flows for which DSMC might be used. It is restricted theoretically to those cases (which

may be only a small fraction of the cells in a hybrid DSMC/EPSM simulation) where the number of collisions per particle per time step is large and hence the distribution function in a cell can be expected to take an equilibrium form. In that case it has been found that EPSM is very efficient compared to DSMC.

It was not the purpose of this work to develop a hybrid DSMC/EPSM code but merely to demonstrate the use of EPSM. To this end, the Taylor Couette flow of a slightly rarefied gas ($Kn = 0.02$ and 0.0133) at high speed ($S_w = 3$) has been calculated using EPSM and DSMC. Differences between DSMC and EPSM results were found and it follows that even at the low Knudsen number of 0.0133 the simulated flow state is non-equilibrium. What is more important than the Knudsen number alone for determining the degree of departure from equilibrium in high speed flows is the product $S_w Kn$ which is the ratio of the characteristic time between collisions and a characteristic time of the macroscopic flow; in the flows considered here this ratio has a value of almost 4% which is apparently enough to produce a significant departure from equilibrium in the simulation. It doesn't appear safe, based on the variation between different DSMC results, to make strong conclusions about Taylor-Couette for the conditions considered here. Great computational effort would need to be expended (particularly on larger numbers of simulator particles but probably also on smaller cell sizes).

EPSM was found to be less sensitive to a change in the number of simulator particles used than was DSMC. There was some indication that EPSM was more dissipative than DSMC, possibly because EPSM was implemented at the cell level, rather than the sub-cell level for which collisions are calculated in DSMC. The question of the accuracy of EPSM in the near continuum regime has been addressed theoretically by considering the nature and magnitude of the effective dissipation and mean free path in EPSM. This analysis serves to emphasize some possible problems in using particle simulation methods (both EPSM and DSMC) in near continuum flows where the usual requirement that the cell size and decoupling interval both be small is relaxed. It that case the dissipation in the simulation methods could depend more on the cell size than on the collision model being used; in this respect the simulation methods become more like continuum solution methods (*e.g.* [15]) which contain an inherent 'artificial' or 'grid' dissipation.

References

[1] G. A. Bird. *Molecular Gas Dynamics.* Clarendon, Oxford, 1976.

[2] G. A. Bird. *Molecular Gas Dynamics and the Direct Simulation of Gas Flows.* Clarendon, Oxford, 1994.

[3] D. B. Hash and H. A. Hassan. A hybrid DSMC/Navier-Stokes solver. A.I.A.A. Paper 95-0410, 1995.

[4] G. A. Bird. Near continuum impact of an under-expanded jet. In *Proc. A.I.A.A. Computational Dynamics Conference*, page 103, New York, 1973. AIAA.

[5] D. I. Pullin. Direct simulation methods for compressible ideal gas flow. *J. Comput. Phys.*, 34:231–244, 1980.

[6] S. Stefanov and C. Cercignani. Monte Carlo simulation of the Taylor-Couette flow of a rarefied gas. *J. Fluid Mech.*, 256:199–213, 1993.

[7] D. I. Pullin. Generation of normal variates with given sample mean and variance. *J. Statist. Comput. Simul.*, 9:303–309, 1979.

[8] K. Nanbu. Direct simulation scheme derived from the Boltzmann equation. I. Monocomponent gases. *J. Phys. Soc. Japan*, 49:2042, 1980.

[9] K. Nanbu. Direct simulation scheme derived from the Boltzmann equation. V. Effects of sample size, number of molecules, step size, and cut-off angle upon simulation data. Technical Report 45-348, Institute of High Speed Mechanics, Tohoko Univ., Japan, 1982.

[10] K. Nanbu. Direct simulation scheme derived from the Boltzmann equation. VI. Velocity correlation in a model cell. *J. Phys. Soc. Japan*, 51:59, 1982.

[11] G. A. Bird. Personal communication, May 1995.

[12] W. G. Vincenti and C. H. Kruger. *An Introduction to Physical Gas Dynamics.* Wiley, New York, 1965.

[13] S. M. Deshpande. Kinetic theory based new upwind methods for inviscid compressible flows. A.I.A.A. Paper 86-0275, 1986.

[14] M. N. Macrossan and R. J. Stalker. Afterbody flow of a dissociating gas down-stream of a blunt nose. A.I.A.A. Paper 87-0407, 1987.

[15] M. N. Macrossan. The equilibrium flux method for the calculations of flows with non-equilibrium chemical reactions. *J. Comput. Phys.*, 80:204, 1989.

[16] M. N. Macrossan, D. I. Pullin, and N. J. Richter. Calculations of three dimensional hypervelocity cone flow with chemical reactions. In *Proc. 10th Aust. Fluid Mech. Conf. Paper 12C-3*, Melbourne, Australia, Dec 1989. University of Melbourne.

[17] M. N. Macrossan. Hypervelocity flow of dissociating nitrogen downstream of a blunt nose. *J. Fluid Mech.*, 207:167, 1990.

[18] M. N. Macrossan and D. I. Pullin. Hypervelocity cone flow with reaction chemistry by a second order kinetic theory based Euler solver. In *Proc. 3rd Australian Supercomputer Conf.*, Melbourne, Australia, Dec 1990. University of Melbourne.

[19] M. N. Macrossan, E. R. Mallett, and D. I. Pullin. Flow calculations for the Hermes Delta wing with a second order kinetic theory based Euler solver. In *Workshop on Hypersonic Flows for Reentry Problems, Part II, Paper C4*, Antibes, France, April 1991. I.N.R.I.A.

[20] M. N. Macrossan and D. I. Pullin. A computational investigation of inviscid hypervelocity flow of a dissociating gas past a cone at incidence. *J. Fluid Mech.*, 266:69–92, 1994.

[21] E. R. Mallett, M. N. Macrossan, and D. I. Pullin. A numerical study of hypersonic leeward flow over a Delta wing using a parallel architecture supercomputer. In *Proc. 11th Aust. Fluid Mech. Conf. (Paper 9D-6)*, pages 1189–1192, Hobart, Australia, Dec 1992. University of Tasmania.

[22] E. R. Mallett, M. N. Macrossan, and D. I. Pullin. Viscous and inviscid hypersonic flow over the Hermes Delta wing. *Workshop on Hypersonic Flows for Reentry Problems, Part III.* Antibes, France. Jan 1993. I.N.R.I.A.

[23] E. R. Mallett, D. I. Pullin, and M. N. Macrossan. Numerical study of hypersonic leeward flow over a blunt nosed delta wing. *A.I.A.A. Journal*, to appear, 1995.

[24] M. N. Macrossan and R. I. Oliver. A kinetic theory solution method for the Navier-Stokes equations. *Int. J. Numer. Meth. Fluids*, 17:177–193, 1993.

[25] J. Davis, R. G. Dominy, J. K. Harvey, and M. N. Macrossan. An evaluation of some collision models used for Monte-Carlo calculation of rarefied hypersonic flows. *J. Fluid Mech.*, 135:355–371, 1983.

[26] M. N. Macrossan. *Diatomic collision models used in the Monte-Carlo direct simulation method applied to rarefied hypersonic flows.* PhD thesis, The University of London, London, England, September 1983.

[27] M. N. Macrossan. Improvements of the algorithms used for Monte-Carlo direct simulation computations. Technical Report 81-03, Department of Aeronautics, Imperial College, London, England, 1981.

Appendices

A The EPSM (equilibrium) algorithm

The core of the EPSM code is the the EQUIL subroutine which establishes equilibrium values for one degree of freedom for a finite sample of particles. The derivation of the method is given in [7] and a description of the algorithm is given in [5]. A more detailed pseudo-code description is given below. Each call of $\mathcal{R}$ returns a new random fraction between 0 and 1 selected from a uniform distribution. The input to the EQUIL subroutine is the number of velocity components to be set N, and the required values of $\bar{u}$ and the variance e'. The output is the set of values $u_j, j = 1, \ldots N$ which are selected from a normal distribution and which satisfy the constraints $\bar{u} = \sum u_j/N$ and $e' = \sum (u_j - \bar{u})^2/2$ (see (8) and (9)). The algorithm may be easier to follow using from the following diagram which illustrates, for particular values of N, the order of generation and interdependence of the various terms in the algorithm.

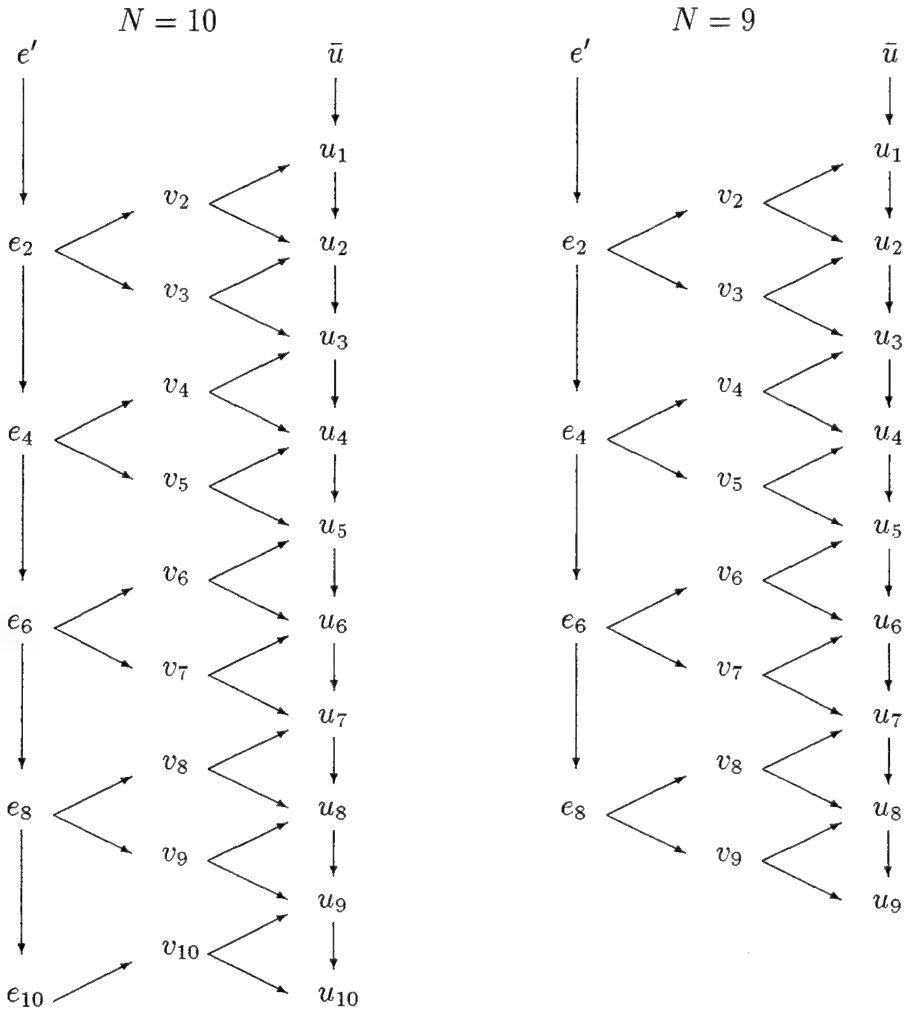

Interdependence of the values e_i, v_j and u_k for $N = 10$ and $N = 9$.

if $N = 2$ then

$u_1 \leftarrow \bar{u} \pm \sqrt{e'}$ (equal probability for $\pm$)

$u_2 \leftarrow 2\bar{u} - u_1$

else if $N = 3$ then

$\theta \leftarrow 2\pi\mathcal{R}$

$v_2 \leftarrow \sqrt{2e'}\cos\theta$

$v_3 \leftarrow \sqrt{2e'}\sin\theta$

$u_1 \leftarrow \bar{u} - \sqrt{2}\, v_2/\sqrt{3}$

$u_2 \leftarrow u_1 + \left(\sqrt{3}\, v_2 - v_3\right)/\sqrt{2}$

$u_3 \leftarrow u_2 + \sqrt{2}\, v_3$

else if $N = 4$ then

$T_1 \leftarrow \mathcal{R}^2$

$e_2 \leftarrow e'(1 - T_1)$

$\theta \leftarrow 2\pi\mathcal{R}$

$v_2 \leftarrow \sqrt{2e_2}\cos\theta$

$v_3 \leftarrow \sqrt{2e_2}\sin\theta$

$u_1 \leftarrow \bar{u} - \sqrt{3}\, v_2/\sqrt{4}v_2$

$u_2 \leftarrow u_1 + \left(\sqrt{4}\, v_2 - \sqrt{2}\, v_3\right)/\sqrt{3}$

$e_4 \leftarrow e'T_1$

$v_4 \leftarrow \pm\sqrt{2e_4}$ (equal probability for $\pm$)

$u_3 \leftarrow u_2 + \left(\sqrt{3}\, v_3 - v_4\right)/\sqrt{2}$

$u_4 \leftarrow u_3 + \sqrt{2}\, v_4$

else if $N > 4$ then

if N is *even* then

$k_{max} \leftarrow N$ /* *maximum index of* e_k */

for $m = 1, \ldots, k_{max}/2 - 1$; step of 1

$T_m \leftarrow \mathcal{R}^{\frac{1}{k_{max}/2-m-0.5}}$

end for

else if N is *odd* then

$k_{max} \leftarrow N - 1$ /* *maximum index of* e_k */

for $m = 1, \ldots, k_{max}/2 - 1$; step of 1

$T_m \leftarrow \mathcal{R}^{\frac{1}{k_{max}/2-m}}$

end for

end if

$e_2 \leftarrow e'(1 - T_1)$

$\theta \leftarrow 2\pi\mathcal{R}$

$v_2 \leftarrow \sqrt{2e_2}\cos\theta$

$v_3 \leftarrow \sqrt{2e_2}\sin\theta$

$u_1 \leftarrow \bar{u} - \sqrt{N-1}\, v_2/\sqrt{N}$

$u_2 \leftarrow u_1 + \left(\sqrt{N}\, v_2 - \sqrt{N-2}\, v_3\right)/\sqrt{N-1}$

continued next page ....

continue general case for $N > 4$ ....

$P \leftarrow 1$ /**initialize the product* $P = \prod_{m=1}^{k/2-1} T_m$ */

for $k = 4, \ldots, k_{max} - 2$; step of 2 /**last value of* e_k, $k = k_{max}$, *is done later* */

$P \leftarrow T_{k/2-1} P$

$e_k \leftarrow e' \left(1 - T_{k/2}\right) P$

$\theta \leftarrow 2\pi\mathcal{R}$

$v_k \leftarrow \sqrt{2e_k} \cos\theta$

$v_{k+1} \leftarrow \sqrt{2e_k} \sin\theta$

$u_{k-1} \leftarrow u_{k-2} + \left(\sqrt{N+3-k}\, v_{k-1} - \sqrt{N+1-k}\, v_k\right) / \sqrt{N+2-k}$

$u_k \leftarrow u_{k-1} + \left(\sqrt{N+2-k}\, v_k - \sqrt{N-k}\, v_{k+1}\right) / \sqrt{N+1-k}$

end for

$P \leftarrow T_{k_{max}/2-1} P$

$e_{k_{max}} \leftarrow e' P$

if N is *even* then

$v_N \leftarrow \pm\sqrt{2e_{k_{max}}}$ (equal probability for $\pm$)

else if N is *odd* then

$\theta \leftarrow 2\pi\mathcal{R}$

$v_{N-1} \leftarrow \sqrt{2e_{k_{max}}} \cos\theta$

$v_N \leftarrow \sqrt{2e_{k_{max}}} \sin\theta$

$u_{N-2} \leftarrow u_{N-3} + \left(\sqrt{4}\, v_{N-2} - \sqrt{2}\, v_{N-1}\right) / \sqrt{(3)}$

end if

$u_{N-1} \leftarrow u_{N-2} + \left(\sqrt{3}\, v_{N-1} - v_N\right) / \sqrt{2}$

$u_N \leftarrow u_{N-1} + \sqrt{2}\, v_N$

end if /*end of general case $N > 4$ */

B Some coding errors in DSMC2A

A number of modifications have been made to the subroutine MOVE2A which calculates the movement of the particles in the axisymmetric flowfield. The most important change concerns the procedures to be followed after a collision with a reflecting surface has been detected. The particle is moved to the collision point by calling subroutine AIFR. The input to AIFR is the initial radial coordinate r (which corresponds to the initial y coordinate in 3D space), the initial radial and tangential velocity components (which correspond to the v_y and v_z velocity components in 3D space), and the position coordinate changes Δy and Δz which occur during the time of flight up until collision with the surface. The output from AIFR is the new radial coordinate and the new radial and tangential velocity components (there is a continuous alteration of the radial and tangential coordinate directions as the particle moves trough 3D space with constant velocity).

The first apparent error in MOVE2A occurs in the call to AIFR when a collision is detected with a surface which is normal to the x axis; AIFR is called with increments Δy and Δz which are appropriate to the time of flight *after* rather than before the collision. The second, and more serious error, concerns the checking of the weighting factors after surface collisions to determine whether the particle (numbered N) should be deleted after collision or duplicate particles should be created. In that the particle numbered N is moved for the time of flight remaining after collision on return from WEIGHT, the code implicitly assumes that the particle was not deleted. If in fact the particle was deleted inside WEIGHT the value of N will have been decremented by 1 and so a lower numbered particle, which will have been moved previously in the given time step, will be moved again.

This, perhaps small, error can lead to a more serious effect. If the first numbered particle $N = 1$ happens to collide with a reflecting surface, and happens to be deleted inside WEIGHT, N will have the value 0 after the return from WEIGHT. The code will attempt to move the non-existent particle $N = 0$; this leads to references to memory locations which are 'out of bounds' of various arrays. To avoid this some extra few lines of code have been added which detect whether the particle was deleted inside WEIGHT; if so the code moves on to the next particle**

Another very small error in the conservation of mass was detected. It was noticed that for the closed flow volume between the two rotating cylinders of the Taylor-Couette flow the total number of particles in the simulation was not constant, even though no weighting factors were used; there was a tiny percentage of simulator particles which were removed from the simulation. To overcome this, a number of small changes were made to the surface collision detection logic. These changes were designed to catch some singular cases when the particle happened to pass exactly (to machine precision) through the end point of a reflecting surface and when the particle finished its flight exactly on the surface. A similar problem occured when a particle would finish its flight just beyond a surface; it one part of the code this would be detected as a valid collision (which it is) but in a subsequent part of the code (because of rounding errors) this case was rejected as a collision and the

**The general axisymmetric code in use at Imperial College for many years [25] [26], which was derived from an early version of the codes now designated G2 in [2], checked weighting factors only when the *final* position of the particle was found. Implementing this strategy in the DSMC2A code is another possible way of avoiding the problem.

particle was left in its position just beyond the surface. Since the surface lay along the boundary of the simulation region the particle was subsequently deleted. A change to 8-byte (double precision) arithmetic when solving a quadratic equation which detects surface collisions seems to have eliminated the known occurrences of this effect.

The detection of multiple reflections from surfaces and boundaries in an axisymmetric flow is a complicated task which was addressed in a report [27] on the 2-D DSMC code which was in use at Imperial College, London. The DSMC2A code has not been checked against all the possible errors mentioned in [27] and there may still be some remaining errors (or some new ones may have been introduced). However, after extensive testing in an enclosed flow with no weighting factors, it has become reasonably clear that any remaining ways for particles to be erroneously deleted are fewer than before. The original frequency of occurrence was small and is smaller now.

An apparent typographical error in the main program (BFND for FND) where a previously computed flow state was read from a file, has been corrected. The extent to which the errors mentioned here may be repeated in other DSMC codes supplied with [2] has not been investigated.

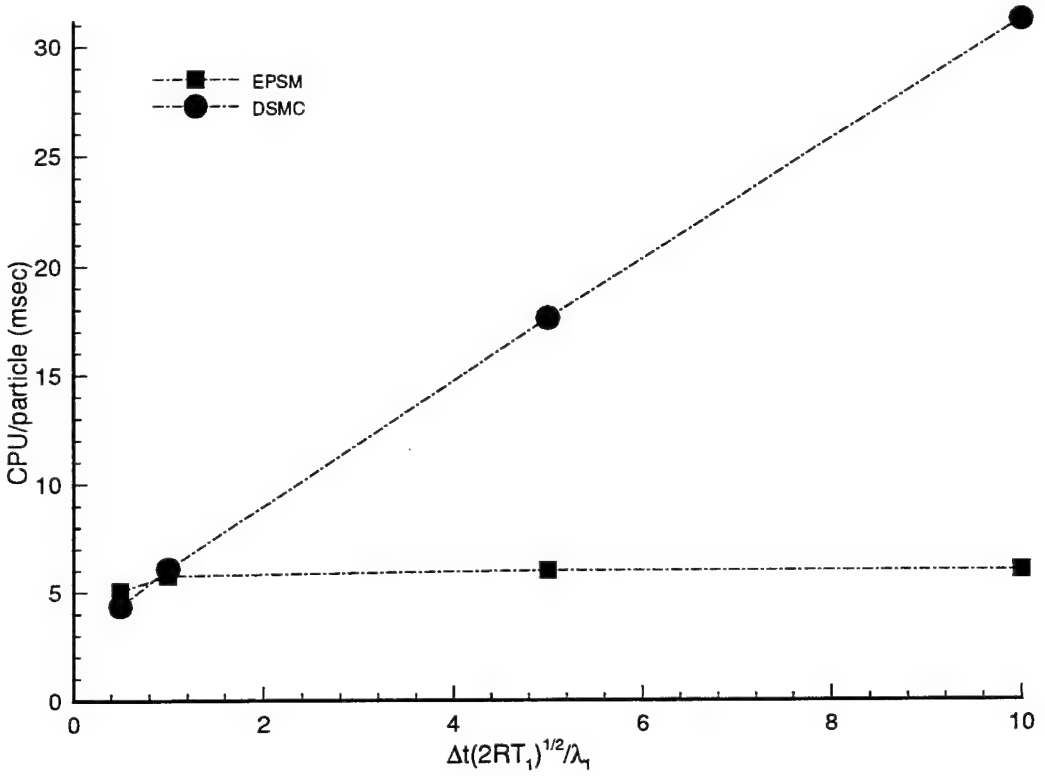

Figure 1: CPU time (SPARCstation 10) required to move 119,124 simulator particles 156 times ($t_{max} = 156\Delta t$), sample the flowfield 52 times, and write the final flow state to disk. Gas at rest between two coaxial stationary cylinders. For DSMC the non-dimensional time step shown on the x-axis is approximately equal to the number of collisions per particle per time step.

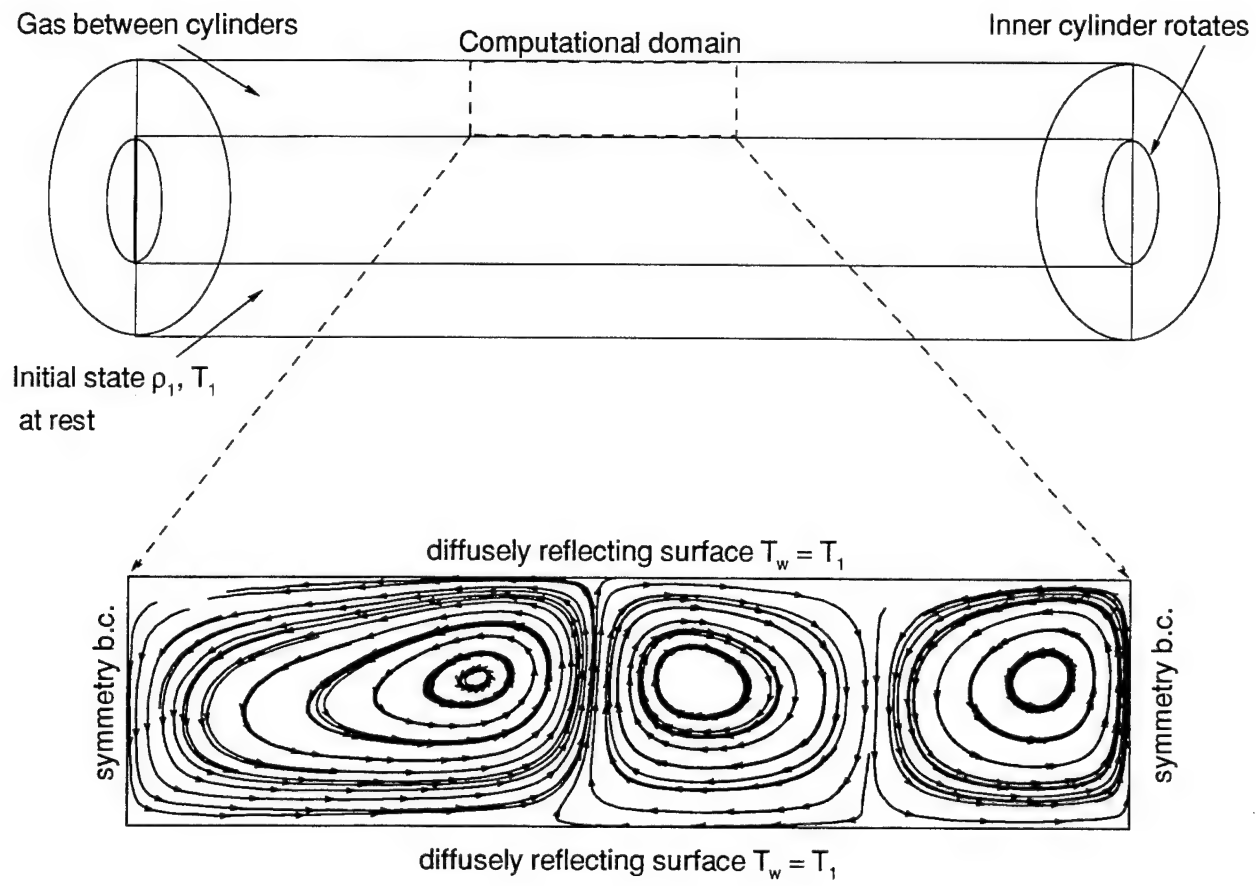

Figure 2: Computational domain and time averaged simulated flow showing toroidal vortices. EPSM. 200x50 grid. $N_{tot} = 119,124$. $\hat{t} = 41 - 60$ revolutions.

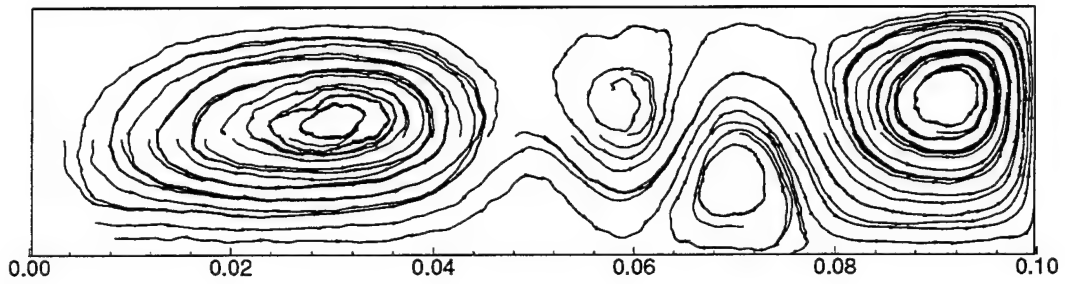

Figure 3: $Kn = 0.02$. 200x50 grid. EPSM. $N_{tot} = 119,124$. $\hat{t} = 5$ revolutions.

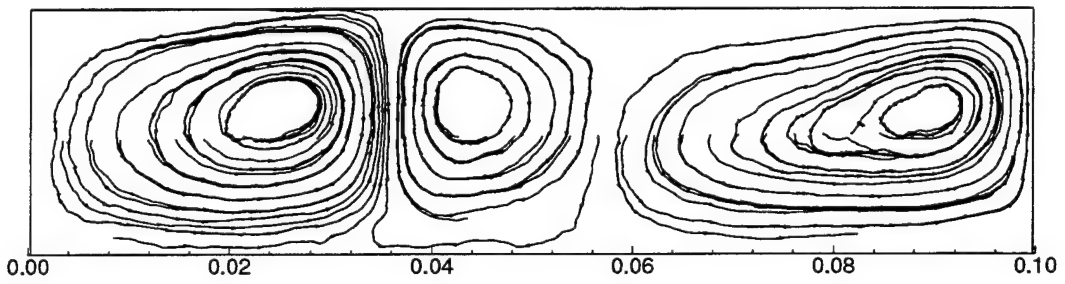

Figure 4: $Kn = 0.02$. 200x50 grid. EPSM. $N_{tot} = 119,124$. $\hat{t} = 10$ revolutions.

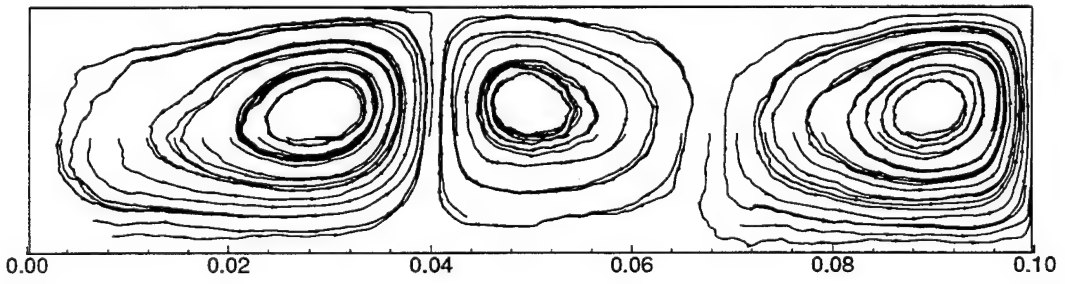

Figure 5: $Kn = 0.02$. 200x50 grid. EPSM. $N_{tot} = 119,124$. $\hat{t} = 20$ revolutions.

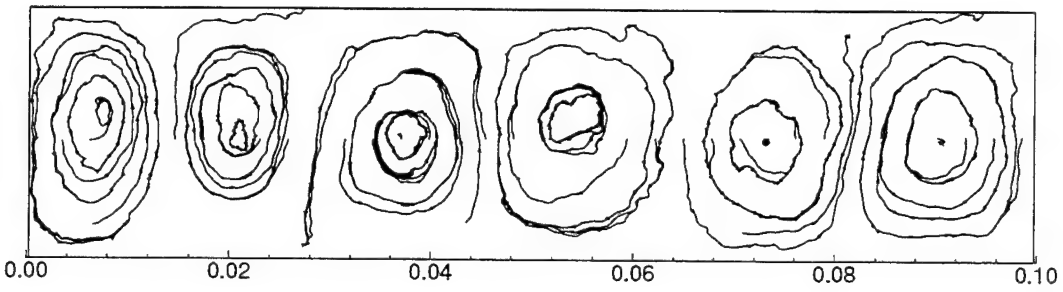

Figure 6: $Kn = 0.02$. 200x50 grid. DSMC. $N_{tot} = 119,124$. $\hat{t} = 5$ revolutions.

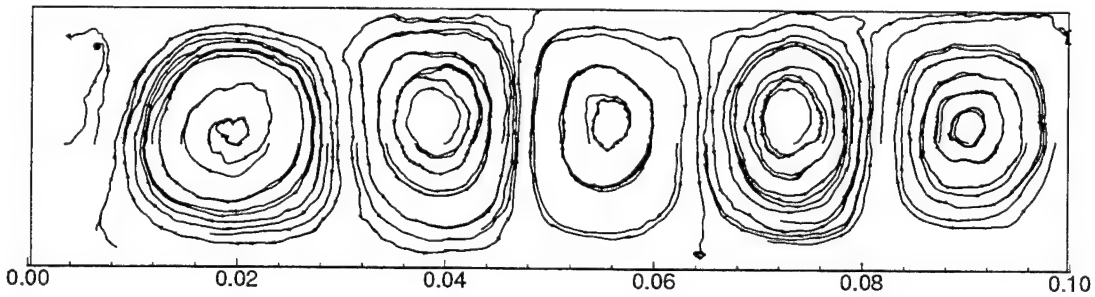

Figure 7: $Kn = 0.02$. 200x50 grid. DSMC. $N_{tot} = 119,124$. $\hat{t} = 10$ revolutions.

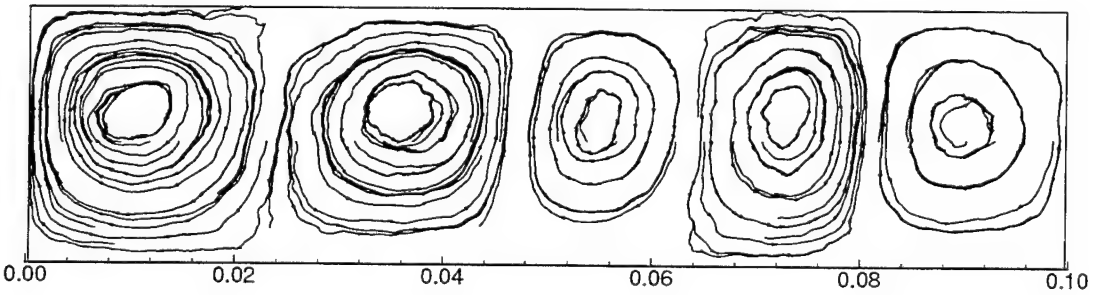

Figure 8: $Kn = 0.02$. 200x50 grid. DSMC. $N_{tot} = 119,124$. $\hat{t} = 20$ revolutions.

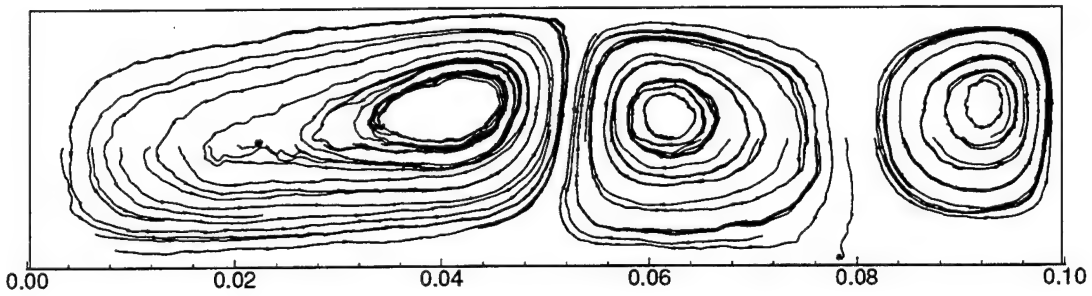

Figure 9: Repeat run with different random numbers. $Kn = 0.02$. 200x50 grid. EPSM. $N_{tot} = 119,124$. $\hat{t} = 20$ revolutions.

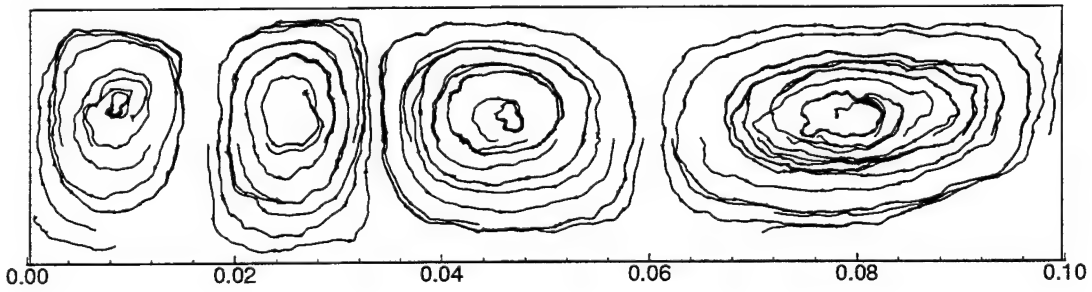

Figure 10: Repeat run with different random numbers. $Kn = 0.02$. 200x50 grid. DSMC. $N_{tot} = 119,124$. $\hat{t} = 20$ revolutions.

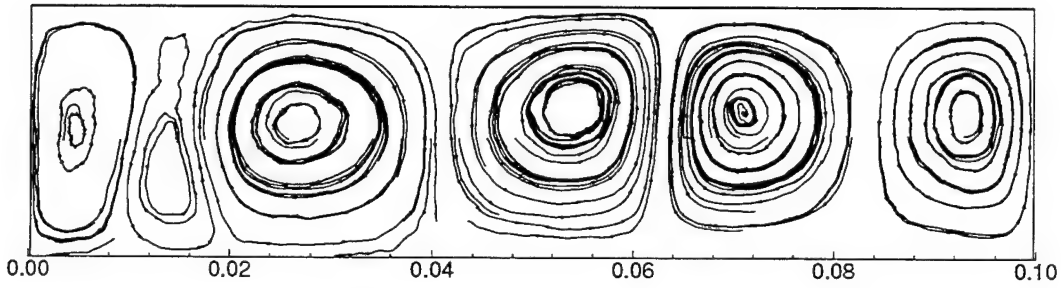

Figure 11: Average of 23 simulator particles/cell. $Kn = 0.02$. 200x50 grid. EPSM. $N_{tot} = 238,248$. $\hat{t} = 10$ revolutions.

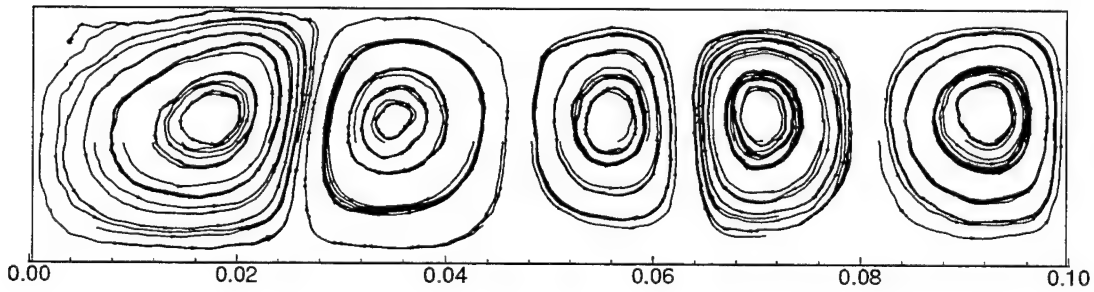

Figure 12: Average of 23 simulator particles/cell. $Kn = 0.02$. 200x50 grid. EPSM. $N_{tot} = 238,248$. $\hat{t} = 10$ revolutions. Repeat run with different random numbers.

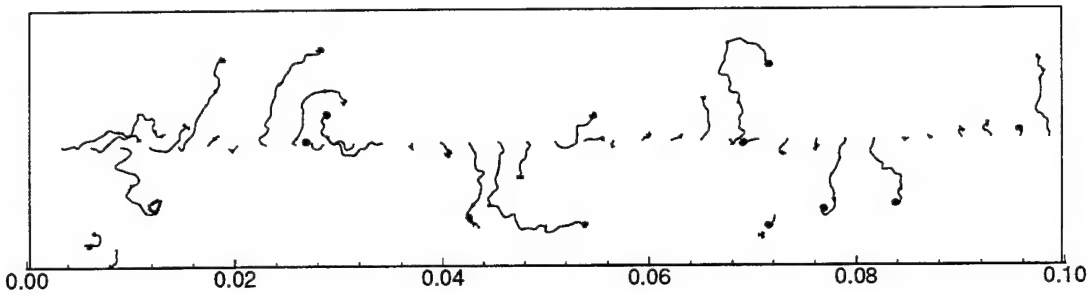

Figure 13: Average of 23 simulator particles/cell. $Kn = 0.02$. 200x50 grid. DSMC. $N_{tot} = 238,248$. $\hat{t} = 10$ revolutions.

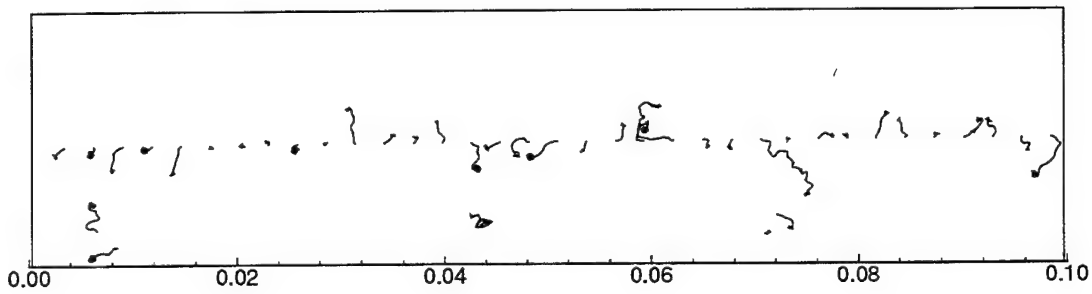

Figure 14: Average of 23 simulator particles/cell. $Kn = 0.02$. 200x50 grid. DSMC. $N_{tot} = 238,248$. $\hat{t} = 10$ revolutions. Repeat run with different random numbers.

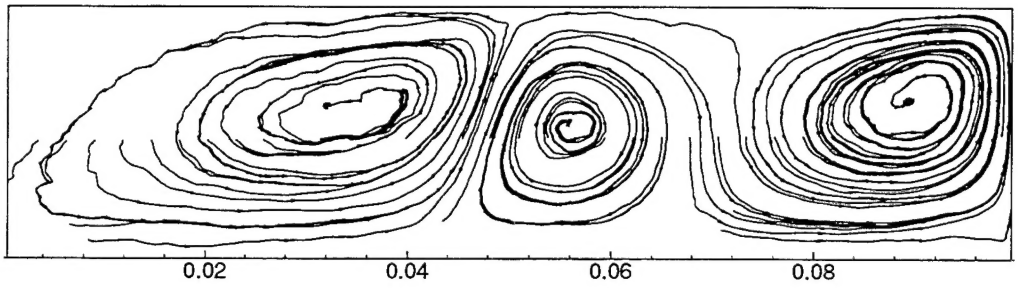

Figure 15: $Kn = 0.0133$. 300x75 grid. EPSM. $N_{tot} = 238,248$. $\hat{t} = 5$ revolutions.

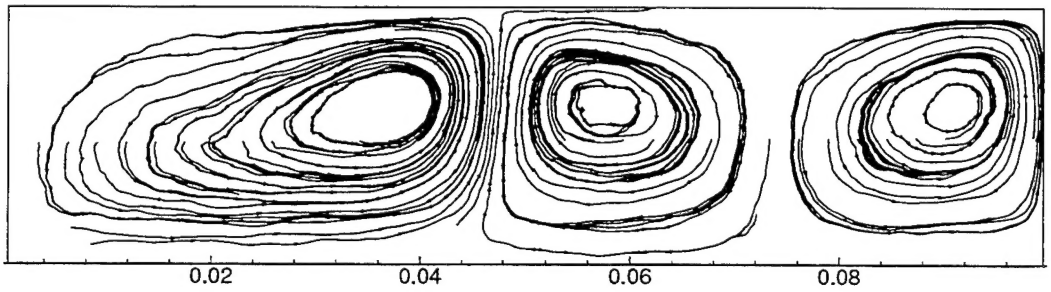

Figure 16: $Kn = 0.0133$. 300x75 grid. EPSM. $N_{tot} = 238,248$. $\hat{t} = 10$ revolutions.

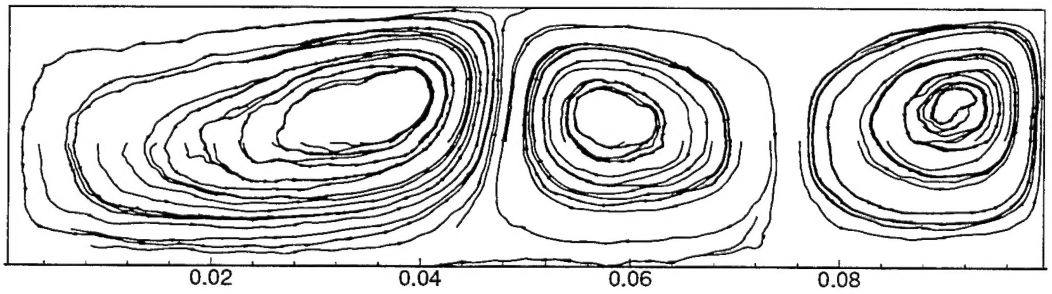

Figure 17: $Kn = 0.0133$. 300x75 grid. EPSM. $N_{tot} = 238,248$. $\hat{t} = 20$ revolutions.

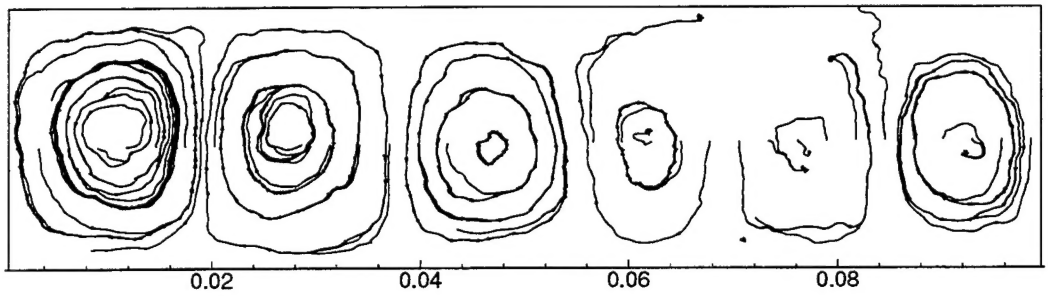

Figure 18: $Kn = 0.0133$. 300x75 grid. DSMC. $N_{tot} = 238,248$. $\hat{t} = 5$ revolutions.

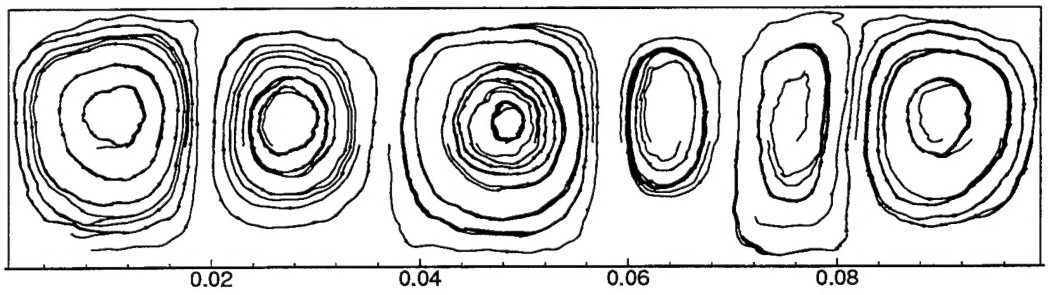

Figure 19: $Kn = 0.0133$. 300x75 grid. DSMC. $N_{tot} = 238,248$. $\hat{t} = 10$ revolutions.

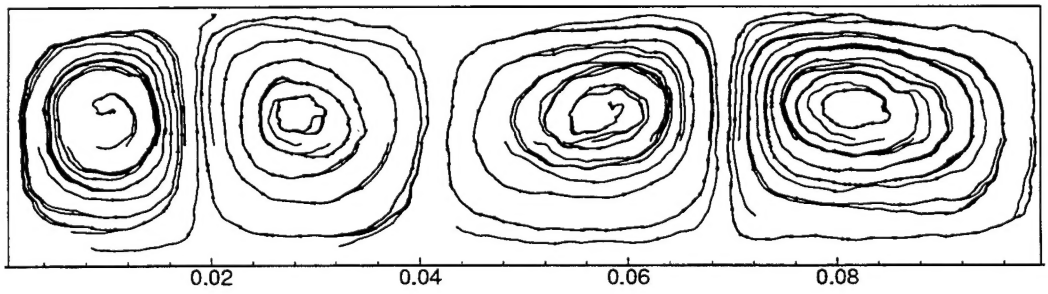

Figure 20: $Kn = 0.0133$. 300x75 grid. DSMC. $N_{tot} = 238,248$. $\hat{t} = 20$ revolutions.

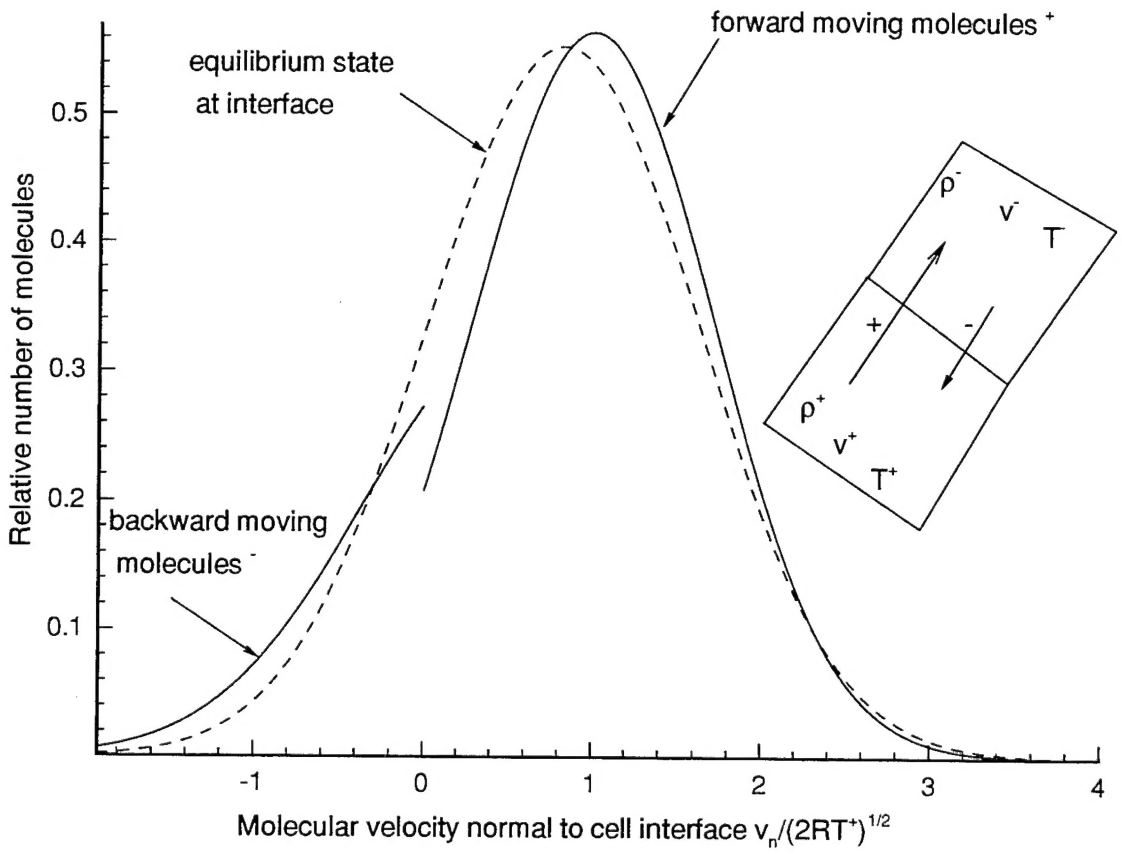

Figure 21: Distribution of c_n for particles crossing the interface between two cells. Solid lines: distribution in EPSM; dashed line: hypothetical equilibrium distribution derived from the EPSM distribution

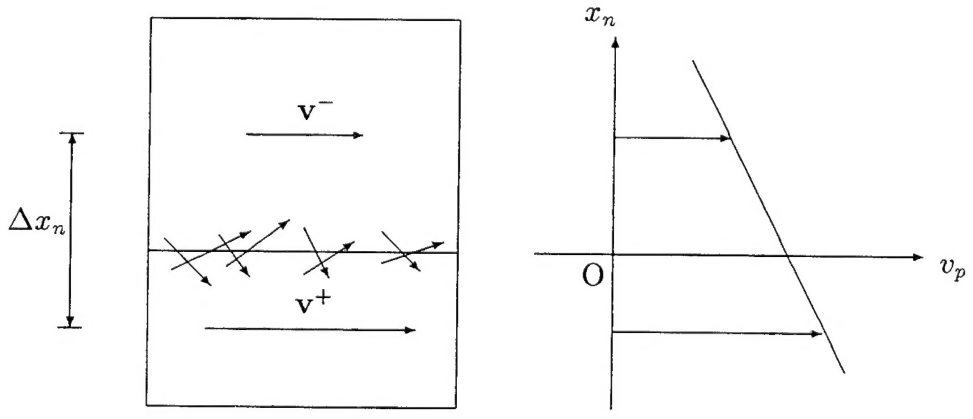

Figure 22: Two cells exchange momentum giving rise to an effective shear stress between them.

REPORT DOCUMENTATION PAGE

Form Approved
OMB No. 0704-0188

Public reporting burden for this collection of information is estimated to average 1 hour per response, including the time for reviewing instructions, searching existing data sources, gathering and maintaining the data needed, and completing and reviewing the collection of information. Send comments regarding this burden estimate or any other aspect of this collection of information, including suggestions for reducing this burden, to Washington Headquarters Services, Directorate for Information Operations and Reports, 1215 Jefferson Davis Highway, Suite 1204, Arlington, VA 22202-4302, and to the Office of Management and Budget, Paperwork Reduction Project (0704-0188), Washington, DC 20503.

1. AGENCY USE ONLY *(Leave blank)*	2. REPORT DATE	3. REPORT TYPE AND DATES COVERED
	June 1995	Contractor Report

4. TITLE AND SUBTITLE
SOME DEVELOPMENTS OF THE EQUILIBRIUM PARTICLE SIMULATION METHOD FOR THE DIRECT SIMULATION OF COMPRESSIBLE FLOWS

5. FUNDING NUMBERS
C NAS1-19480
WU 505-90-52-01

6. AUTHOR(S)
M. N. Macrossan

7. PERFORMING ORGANIZATION NAME(S) AND ADDRESS(ES)
Institute for Computer Applications in Science
and Engineering
Mail Stop 132C, NASA Langley Research Center
Hampton, VA 23681-0001

8. PERFORMING ORGANIZATION REPORT NUMBER
ICASE Interim Report No. 27

9. SPONSORING/MONITORING AGENCY NAME(S) AND ADDRESS(ES)
National Aeronautics and Space Administration
Langley Research Center
Hampton, VA 23681-0001

10. SPONSORING/MONITORING AGENCY REPORT NUMBER
NASA CR-198175
ICASE Interim Report No. 27

11. SUPPLEMENTARY NOTES
Langley Technical Monitor: Dennis M. Bushnell
Final Report

12a. DISTRIBUTION/AVAILABILITY STATEMENT
Unclassified–Unlimited

Subject Category 59

12b. DISTRIBUTION CODE

13. ABSTRACT *(Maximum 200 words)*

The direct simulation Monte Carlo (DSMC) method is the established technique for the simulation of rarefied gas flows. In some flows of engineering interest, such as occur for aero-braking spacecraft in the upper atmosphere, DSMC can become prohibitively expensive in CPU time because some regions of the flow, particularly on the windward side of blunt bodies, become collision dominated. As an alternative to using a hybrid DSMC and continuum gas solver (Euler or Navier-Stokes solver) this work is aimed at making the particle simulation method efficient in the high density regions of the flow. A high density, infinite collision rate limit of DSMC, the Equilibrium Particle Simulation method (EPSM) was proposed some 15 years ago. EPSM is developed here for the flow of a gas consisting of many different species of molecules and is shown to be computationally efficient (compared to DSMC) for high collision rate flows. It thus offers great potential as part of a hybrid DSMC/EPSM code which could handle flows in the transition regime between rarefied gas flows and fully continuum flows. As a first step towards this goal a pure EPSM code is described. The next step of combining DSMC and EPSM is not attempted here but should be straightforward. EPSM and DSMC are applied to Taylor-Couette flow with $Kn = 0.02$ and 0.0133 and $S_w = 3$). Toroidal vortices develop for both methods but some differences are found, as might be expected for the given flow conditions. EPSM appears to be less sensitive to the sequence of random numbers used in the simulation than is DSMC and may also be more dissipative. The question of the origin and the magnitude of the dissipation in EPSM is addressed. It is suggested that this analysis is also relevant to DSMC when the usual accuracy requirements on the cell size and decoupling time step are relaxed in the interests of computational efficiency.

14. SUBJECT TERMS
Direct Simulation; Near Continuum Flow; Effective Dissipation

15. NUMBER OF PAGES
34

16. PRICE CODE
A03

17. SECURITY CLASSIFICATION OF REPORT	18. SECURITY CLASSIFICATION OF THIS PAGE	19. SECURITY CLASSIFICATION OF ABSTRACT	20. LIMITATION OF ABSTRACT
Unclassified	Unclassified		

NSN 7540-01-280-5500

Standard Form 298(Rev. 2-89)
Prescribed by ANSI Std. Z39-18
298-102